Analytical Overvoltage and Power-Sharing Control Method for Photovoltaic-Based Low-Voltage Islanded Microgrid

Bakhshi-Jafarabadi, Reza; Lekic, Aleksandra; Marvasti, Farzad Dehghan; De Jesus Chavez, Jose; Popov, Marjan

DOI
10.1109/ACCESS.2023.3336945

Publication date
2023

Document Version
Final published version

Published in
IEEE Access

IEEE Access
Multidisciplinary | Rapid Review | Open Access Journal

Received 3 November 2023, accepted 21 November 2023, date of publication 27 November 2023,
date of current version 4 December 2023.

Digital Object Identifier 10.1109/ACCESS.2023.3336945

RESEARCH ARTICLE

Analytical Overvoltage and Power-Sharing Control Method for Photovoltaic-Based Low-Voltage Islanded Microgrid

REZA BAKHSHI-JAFARABADI[1], (Member, IEEE), ALEKSANDRA LEKIĆ[1], (Senior Member, IEEE), FARZAD DEHGHAN MARVASTI[1], (Member, IEEE), JOSE DE JESUS CHAVEZ[2], (Senior Member, IEEE), AND MARJAN POPOV[1], (Fellow, IEEE)

[1]Delft University of Technology, Faculty of EEMCS, 2628CD Delft, The Netherlands
[2]School of Engineering and Sciences, Tecnologico de Monterrey, Monterrey, Nuevo Leon 64849, Mexico

Corresponding author: Reza Bakhshi-Jafarabadi (Reza.Bakhshi@tudelft.nl)

ABSTRACT Overvoltage instability is a growing concern in a standalone low-voltage (LV) microgrid (MG) with non-dispatchable intermittent renewable energies such as residential and commercial photovoltaic generators (PVGs). Several overvoltage controllers used in PV arrays have adopted the concept of standard deviation from the maximum power point (MPP) to curtail the generated power. However, these solutions lack presenting analytical expression for the MPP deviation size, settings tuning independent of the MG's/PV's characteristics, scalability, and accurate power-sharing in the same control structure. To overcome these limitations, this paper proposes a new analytical MPP tracking (MPPT)-based overvoltage and power-sharing control method using the series equivalent resistance of the PV module model. By applying this analytical expression, the size of the PV array voltage shift to the right-hand side of the MPP is obtained in terms of overvoltage level, while all PVGs proportionally curtail the active power output. The effectiveness of the proposed methodology is shown in various low-demand and high-PV generation cases through a real time digital simulator (RTDS) platform. In addition to the fast and accurate performance, the presented method benefits from the straightforward and communication-free structure as it solely exploits the point of common coupling (PCC) voltage. Also, the method's threshold does not require re-tuning after MG restructure, ensuring scalability. Without relying on other microgrid facilities, the proposed methodology is accordingly an effective solution for practical PV-based LV MGs.

INDEX TERMS Analytical overvoltage control, islanded microgrid (MG), maximum power point tracking (MPPT), photovoltaic generator (PVG).

NOMENCLATURE

Acronyms

BESS	Battery energy storage system
DG	Distributed generator
LC	Load control
LV	Low-voltage
MG	Microgrid
MGCC	Microgrid central control
MPP	Maximum power point
MPPT	Maximum power point tracking
OC	Open-circuit
P&O	Perturb and observe
PCC	Point of common coupling
PVG	Photovoltaic generator
PWM	Pulse width modulation
RTDS	Real time digital simulator
STC	Standard test condition
VSI	Voltage source inverter

The associate editor coordinating the review of this manuscript and approving it for publication was Alon Kuperman.

Units

a	Diode ideally constant
I_{ph}	Photocurrent of PV single-diode model
I_{PV}	PV array current
I_0	Reverse saturation current of diode
P_{NEW}	PVG active power output after curtailment
P_{PV}	PV array power
P_{PVG}	PVG active power output
R_P	Parallel resistance of PV single-diode model
R_S	Series resistance of PV single-diode model
V_{MPP}	PV array voltage at MPP
V_{NEW}	New V_{PV} after method's disturbance injection
V_{OC}	Open-circuit PV array voltage
$V_{PCC,nom}$	Nominal PCC voltage
V_{PV}	PV array voltage
V_T	Thermal voltage
α	Control parameter for power curtailment
β	$(V_{OC}/V_{MPP}) - 1$
ΔP_{PVG}	PVG active power curtailment
ΔV_{PCC}	Overvoltage level at PCC

I. INTRODUCTION

A. BACKGROUND AND MOTIVATION

Microgrid is a self-contained small-scale network comprising distributed generations (DGs), local demands, and storage systems. This low-voltage (LV) grid provides deeper penetration of inverter-based renewable energies with several techno-economic and environmental benefits [1]. With this substantial penetration, however, the electricity supply is volatile, and the MG lacks power inertia, causing instability even with a small disturbance [2]. In addition, new standards emphasize uninterruptable electricity supply of priority loads even when the utility is out of service, e.g., IEEE Standard 1547.1-2020 for photovoltaic generators (PVGs) [3].

To meet these requirements and characteristics, the development of new control strategies to ensure MG's secure and resilient supply has drawn great attention [4]. The main goal is to balance the active and reactive powers between generation and consumption. The load demand should also be shared proportionally among the DGs to limit voltage and frequency variation at different buses. To this end, hierarchical control schemes, including primary, secondary, and tertiary, have been presented [5]. Fig. 1 illustrates this hierarchical architecture for a PV-based MG with a battery energy storage system (BESS) connected at N^{th} point of common coupling (PCC), i.e., PCC_N. Connected loads and DGs to the PCCs are shown by L_1–L_N and DG_1–DG_N, respectively.

At the first control level, the voltage and frequency at the PCC are quickly stabilized by primary schemes [6]. Based on the measured variables at PCC, the local controller (LC) determines the instructions for DGs, BESS, or loads connected to that particular PCC. According to the deployment of the communication channel between LCs, shown by red dashed lines in Fig. 1, the primary controllers are divided into two groups. Non-communication controllers have only exploited the data of a given PCC [7]. Among existing communication-free solutions, droop control is widely applied to regulate the DGs' output current at the preset ratio. Apart from simple structure, these schemes cannot support voltage control and power-sharing simultaneously. In communication-based schemes such as centralized [8], master-salve [9], and distributed [10], the nearby LCs exchange PCC data, e.g., a two-layer distributed controller in [10]. The physical layer employs a conventional droop controller with an additional error signal defined in the cyber layer. This extra signal minimizes voltage deviation and power-sharing errors simultaneously. Besides, the required communication infrastructure is mitigated as the pinned DGs to a given bus are controlled by the same signal.

Since most droop techniques cannot fully control voltage/frequency, secondary schemes have been adopted to amend residue voltage/frequency deviation from the setpoints [11]. Data of all PCCs are measured and sent to the microgrid central control (MGCC) to compute and send the instructions to the individual DGs, BESS, and loads. In tertiary plans, MGCC fulfills the optimum economic dispatch and MG synchronization at a high level [12]. Although the tertiary and secondary schemes effectively enhance the MG control from a techno-economic perspective, they suffer from high-cost and time-consuming re-setting of the MGCC when a DG is added up or disconnected. Moreover, relying on MGCC solely alleviates the scheme's reliability, i.e., the control is lost when MGCC fails. To overcome these problems, a combination of primary, secondary, and tertiary schemes has been recommended in hybrid plans to accomplish different control goals [13]. Apart from outstanding performance, high burden cost and complex structure are the main shortcomings.

Finally, machine learning tools have been suggested at all control levels, mainly primary, to develop new schemes. Reference [14] presented a data-driven neural network-based droop controller for the power-sharing of DGs, supported by BESS for MG's power balance. As shown in hardware-in-the-loop simulations, this work expedites the transient performance compared with conventional droop controllers.

B. LITERATURE REVIEW OF OVERVOLTAGE CONTROL SCHEMES

Overvoltage instability is a growing concern in a standalone LV MG with non-dispatchable intermittent PVGs. With a high R/X of short feeders, MG voltage is more sensitive to the active power than the reactive one; thus, overvoltage occurs during underloading conditions [15]. According to the International Energy Agency report, 25% and 23% of the global grid-tied PVG installation in 2022 was realized by the commercial and residential sectors, respectively [16]. This large share of residential and commercial PV systems implies a wide range of applications for the overvoltage issue in LV isolated MGs. Active power curtailment strategy has been widely adopted by PVGs to amend this surplus power [17], [18], [19], [20], [21], [22], [23]. Other works presented

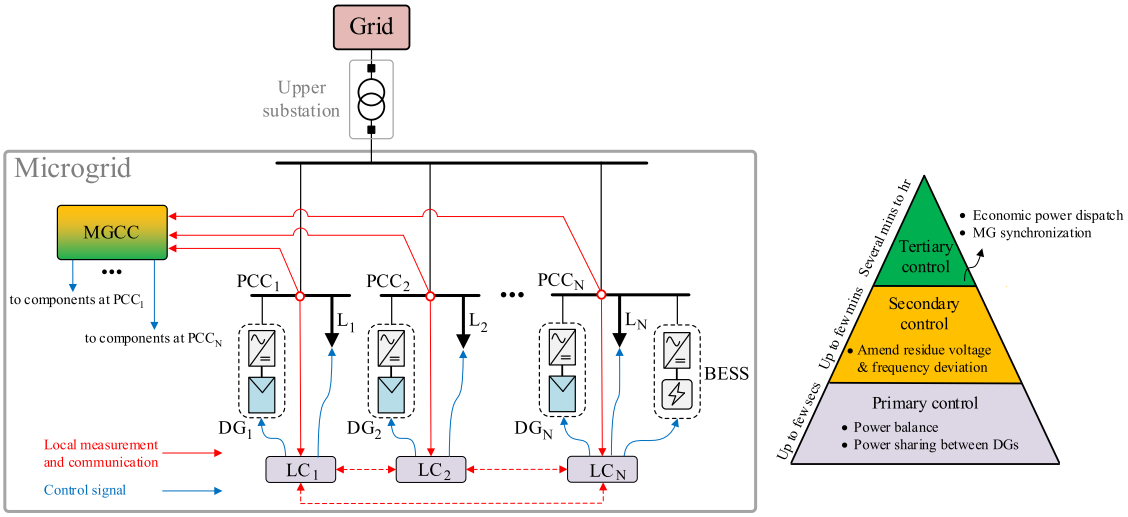

FIGURE 1. Hierarchical control structure in the islanded microgrid.

a coordinated control of BESS and PVG [24], [25], [26], [27], [28] whilst active loads plug-in has been proposed in [29].

A comprehensive survey of existing BESS-based control solutions for isolated MG has been reported in [24]. From the technical perspective, the main focus is to develop an output voltage control by PV and BESS with a seamless transition between surplus and deficit power conditions, respectively [25]. In addition to this fast performance, this combination has been used to regulate the voltage in a larger time-step, within a day [26]. Also, some researchers designed PVG+BESS controllers to mitigate the required communication burden, using an event-triggered approach [27]. Finally, other works optimized voltage regulation and precise power-sharing with a techno-economic objective, e.g., minimum BESS cost, maximum BESS lifetime, and minimum BESS efficiency degradation [28].

As an economical solution, overvoltage can be resolved from the generator side without dependency on other facilities. The output power of the PVG relies on the outdoor conditions, mostly irradiance and temperature; hence, the voltage source inverter (VSI) uses the maximum power point tracking (MPPT) algorithm to extract the maximum available power. When LV MG lacks active power, MPPT is applied and power shortage is balanced by either discharging BESS or load shedding [30]. In an underloaded MG, the PV array's power is curtailed in VSI to mitigate the power mismatch. As shown in Fig. 2, the curtailed power can be used as a reserve to meet the probably raised load.

According to these control modes, i.e., MPPT and MPPT-OFF (voltage control), two separate controllers have been designed. The most effort on existing methods is first to detect the PV array's operating point, and then provide a seamless transition from MPPT to the voltage control mode and vice versa. In this context, the slope of PV power (P_{PV}) vs. voltage (V_{PV}) has been used in [18] to determine its operating point, i.e., $\mathrm{d}P_{PV}/\mathrm{d}V_{PV} > 0$ and $\mathrm{d}P_{PV}/\mathrm{d}V_{PV} < 0$ for left- and right-hand side of MPP, respectively (Fig. 2). Through a mode switch index in DC/DC converter, the PV array moves toward and away from MPP to compensate for the deficit and surplus power, respectively. The conventional droop controller is also embedded in the DC/AC converter to further support the MG in power shortage situations. Apart from the promising results, the controller's transfer functions highly depend on converters' control gains and parameters. A modified MPPT algorithm has been developed in [19] to manipulate the overvoltage of a DC MG. This work provides a smooth transition from MPPT to voltage control mode without applying a communication link. However, since it is defined only for an MG with a single PVG, it does not support the power-sharing of multi-PV units. Reference [20] shifted the droop curve of the PV system to change its active power output in terms of load demand. As mentioned by the authors, the required PV array's voltage shift to fulfill this active power change has not been defined analytically. Hence, the PV active power output tracks a reference through a PI controller. In [21], a reference power has been defined for the modified perturb and observe (P&O) MPPT algorithm so that the PV power balances the load. The neural network has also been applied to shift the PV array's operating point between its MPP (V_{MPP}) and open-circuit voltage (V_{OC}), ensuring its stable performance. The size of the PV array voltage shift to track the reference power has been determined in the neural network training process by MATLAB simulations. Another study defined two PV unit operation modes: grid-connected and islanded operation with MPPT and constant power control modes [22]. Similar to [18], the authors exploited $\mathrm{d}P_{PV}/\mathrm{d}V_{PV}$ criterion to decide the direction of the PV array voltage shift.

Although there are several effective MPPT-based voltage controllers in the literature, they suffer high costs, complex

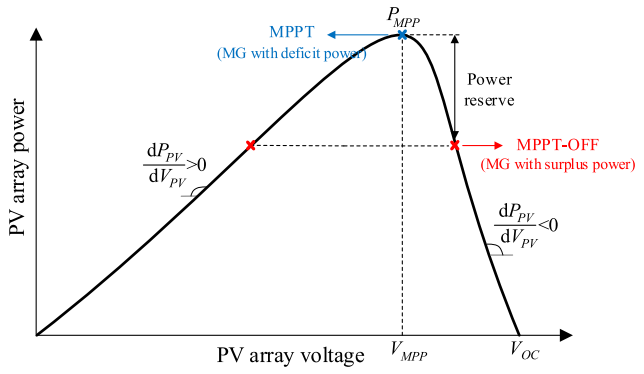

FIGURE 2. MPPT-OFF controller in overvoltage conditions.

implementation [21], and dependency on the parameters of the studied case [18], [19], [21], [22], limiting their practical application. Furthermore, these schemes do not provide analytical expressions for the size of PV array voltage change to support the power mismatch [18], [19], [20], [21], [22]. Finally, most methods have presented two separate control loops for MPPT and voltage control mode, whilst a seamless transition is realized through a switching control, jeopardizing the method's reliability [17], [18], [19], [20], [21], [22], [23].

C. CONTRIBUTIONS AND PAPER STRUCTURE

According to the literature, the development of an accurate overvoltage and power-sharing control with minimum dependency on MG's and PV's characteristics, simple structure, and communication independence is still of interest. Furthermore, the required power curtailment has yet to be quantified analytically. To this end, this paper proposes an analytical overvoltage and power-sharing control method for PV-based LV MG. These aims are achieved by deviating the PV array voltage from the MPP, using PCC voltage data. In addition to the precise PV power curtailment to boost the overvoltage stability margin, this method provides several advantages, including:

- The size of the PV array voltage shift is analytically determined, irrespective of the PV's and MG's settings. Hence, it can be simply developed into a new system.
- The active power curtailment is proportionally defined for all PV units so that the optimum power-sharing of multiple generators is ensured.
- The PV array voltage shift is the only setting of the proposed method that does not need re-tuning after a PVG is added or removed. Thus, the scalability of the proposed method is guaranteed.
- Its structure is straightforward and inexpensive.
- Since it exploits solely the PCC voltage information, i.e., no communication link is applied with other facilities, it is markedly reliable.

The rest of the paper is organized as follows. Section II elaborates on the proposed analytical overvoltage and power-sharing controller. Section III details an LV MG with two commercial PV systems as a standard case study system. Afterward, the authenticity of the presented method is evaluated in a real time digital simulator (RTDS) under various overvoltage scenarios in single and multi-PVG MG. The overall outstanding performance of the recommended method is highlighted in Section V through its comparison with a few recent source-driven MPPT-based schemes. Finally, concluding remarks are given in Section VI.

II. PROPOSED METHODOLOGY DESCRIPTION

Balanced condition is the normal operation mode of the MG. In addition, two operating modes occur for the MG according to its power mismatch:

- Undervoltage: Total load demand exceeds all PV units' generation. This situation is controlled by BESS dis-

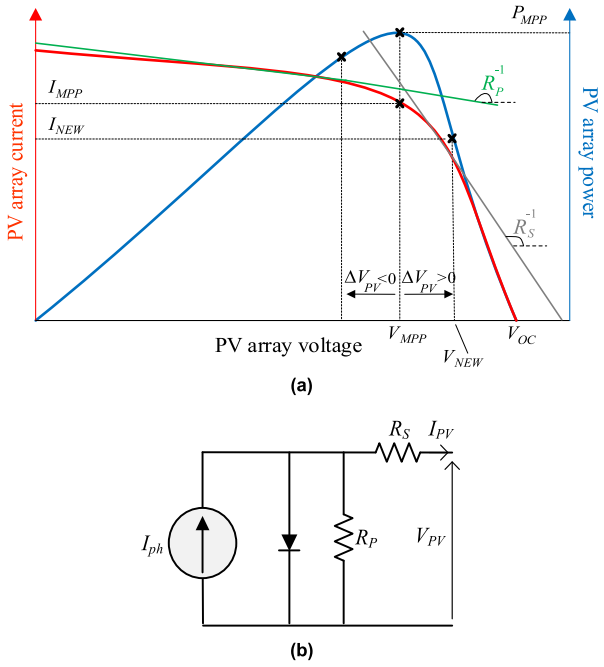

FIGURE 3. Proposed PV generator power curtailment methodology: a) Relation of new, open-circuit, and MPP operating points of PV module, b) Series resistance in the single-diode model of PV model.

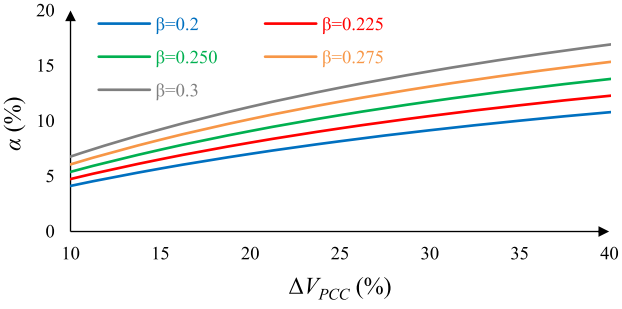

FIGURE 4. PV array voltage deviation from MPP to control overvoltage.

charge or load shedding; thus, the PVG works in MPPT mode, and no further support is expected.
- Overvoltage: Total generation is larger than MG's consumption. In this condition, curtailment of the PVG amends the MG's surplus power, and PCC voltage restores within the tolerable range.

Based on the latter case, the main idea of the proposed method is to change the PV array voltage analytically so that the active power output drops. To this end, the relation of the PVG active power output before curtailment (P_{PVG}) and an overvoltage ($V_{PCC,nom} + \Delta V_{PCC}$) in an islanded LV MG can be expressed as follows:

$$P_{PVG} = P_{MPP} = \frac{(V_{PCC,nom} + \Delta V_{PCC})^2}{R_L} \tag{1}$$

where R_L stands for the resistance part of the equivalent constant impedance at PCC and $V_{PCC,nom}$ is the nominal voltage. It is worth mentioning that by neglecting the VSI's losses, P_{PVG} equals the MPP power (P_{MPP}) before employing the proposed strategy. By assuming ΔP_{PVG} as the required power drop to restore PCC voltage to the nominal level, one obtains:

$$P_{MPP} - \Delta P_{PVG} = \frac{V_{PCC,nom}^2}{R_L} \tag{2}$$

Combining (1) and (2) results in:

$$\frac{\Delta P_{PVG}}{P_{MPP}} = 1 - (\frac{1}{1 + \Delta V_{PCC}})^2 \tag{3}$$

Recent expression is obtained by considering $V_{PCC,nom} = 1$ pu. Equation (3) shows the required active power curtailment to decline PCC voltage from $1+\Delta V_{PCC}$ to 1 pu. Note that these equations are valid for LV MGs with high R/X ratios.

As mentioned earlier, in normal and undervoltage conditions, the PV array voltage is adjusted by the MPPT algorithm to harvest the maximum power ($P_{PVG} = P_{MPP}$), and no further control is expected from the PVG. In an overvoltage case ($\Delta V_{PCC} > 0$), however, MPPT is disabled, and V_{PV} is shifted to a new set point (V_{NEW}):

$$V_{NEW} = V_{MPP} + \Delta V_{PV} \tag{4}$$

where ΔV_{PV} is the PV array voltage shift. It should be noted that although the PV array power lessens for both positive and negative ΔV_{PV}, a greater reduction is attained in the right-hand side of MPP for a given ΔV_{PV} (Fig. 3 (a)). Thus, this parameter is chosen positively ($\Delta V_{PV} > 0$) in the current work.

The proposed analytical power-sharing-based overvoltage control is described using the slope of the PV array's power vs. voltage on the right-hand side of MPP. For a better understanding of the methodology, this slope is represented by series equivalent resistance (R_S) in the PV array single-diode model, shown in Fig. 3 (b). Considering the PV module single-diode model, its current (I_{PV}) vs. V_{PV} can be expressed as follows [19]:

$$I_{PV} = I_{ph} - I_0[\exp \frac{V_{PV} + R_S I_{PV}}{V_T a}] - (\frac{V_{PV} + R_S I_{PV}}{R_P}) \tag{5}$$

where I_{Ph}, I_0, V_T, and a are photocurrent, reverse saturation current of the diode, thermal voltage, and diode ideally constant, respectively. The R_S and parallel resistance (R_P) are also modeled to represent the right- and left-hand side of MPP, respectively (Fig. 3 (a)). According to the slope of MPP's right-hand side ($1/R_S$), the relation of NEW, MPP, and open-circuit (OC) operating points can be given as:

$$R_S = \frac{V_{NEW} - V_{OC}}{I_{NEW}} = \frac{V_{MPP} - V_{OC}}{I_{MPP}} \tag{6}$$

By considering αV_{MPP} as the PV array voltage shift, i.e., $V_{NEW} = (1+\alpha)V_{MPP}$, (6) can be rewritten as follows:

$$I_{NEW} = I_{MPP} \frac{(\beta - \alpha)}{\beta} \tag{7}$$

where $\beta = (V_{OC}/V_{MPP})$-1 and lies inside the 0.2–0.3 range. This parameter can be computed simply by the PV module information at standard test condition (STC), provided by the manufacturer in its datasheet [31]. The PV array power at the new operating point (P_{NEW}) can be determined by multiplying (7) into V_{NEW}, i.e., $P_{NEW} = V_{NEW} I_{NEW}$:

$$P_{NEW} = V_{MPP}(1+\alpha) I_{MPP}(\frac{\beta - \alpha}{\beta}) = P_{MPP}(1+\alpha)(\frac{\beta - \alpha}{\beta}) \tag{8}$$

The PV array power curtailment ($\Delta P_{PVG} = P_{MPP}$–P_{NEW}) can be finally deducted as follows:

$$\Delta P_{PVG} = P_{MPP}(\alpha^2 \beta^{-1} - \alpha + \alpha \beta^{-1}) \tag{9}$$

In the recent equation, α can be defined so that the required power mismatch is compensated by the PVG. Thence, the MG voltage is re-established to the nominal setting. By considering (3) and (9), the final expression is derived as:

$$\alpha^2 \beta^{-1} - \alpha + \alpha \beta^{-1} = 1 - (\frac{1}{1 + \Delta V_{PCC}})^2 \tag{10}$$

Therefore, (10) analytically computes the required PV array deviation from MPP in terms of β and ΔV_{PCC}. Note that solving (10) gives two positive and negative real roots, i.e., $\alpha \geq 0$ and $\alpha < 0$, implying the solutions for the PV array shift to the MPP's right- ($\Delta V_{PV} > 0$) and left-hand side ($\Delta V_{PV} < 0$), respectively. As noted earlier, since a given power curtailment can be reached with smaller ΔV_{PV} in the MPP's right-hand side, the positive root is chosen for PV array voltage shift ($\alpha V_{MPP} \geq 0$). Equation (10) can be solved offline for various sets of β and overvoltage. The computed results are shown in Fig. 4 for $\alpha \geq 0$. Hereby, once β is defined from the information of the PV module datasheet, α can be computed in terms of overvoltage level. This implies a straightforward application of the proposed methodology in practice.

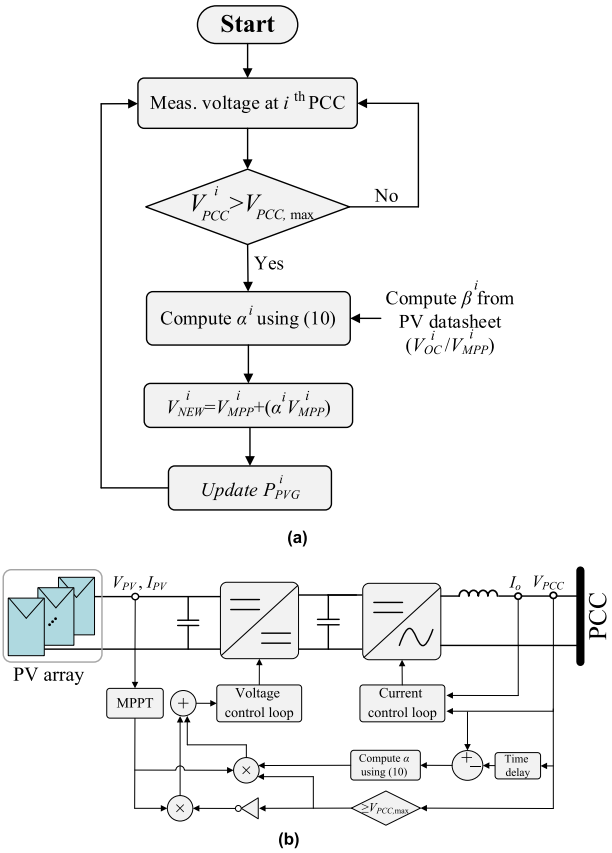

FIGURE 5. Proposed overvoltage control: a) Flowchart, b) Realization in two-stage VSI.

It is worth mentioning that the proposed analytical method in (4), (6)–(10) are valid for all PV modules, irrespective of the employed technology and size.

The flowchart and realization of the presented controller for a two-stage VSI are depicted in Fig. 5. In these figures, I_o represents the PVG's AC output current. Also, $V_{PCC,\max}$ is the maximum PCC voltage limit wherein the presented method is activated. Furthermore, the time delay block is chosen concerning the MG's frequency, e.g., in this work, 20 ms for the studied case with 50 Hz frequency. It is seen that the proposed technique includes *1)* PCC voltage measurement and comparison with maximum permissible limit, *2)* computing α from (10), and *3)* injecting the disturbance into PV array voltage. Measurement, comparison and solving (10), and disturbance injection are implemented by a sensor, microcontroller/digital signal processor, and signal generator, respectively. According to this inexpensive and straightforward structure without employing a communication link, it can be simply integrated into the existing PV-based LV MGs. What's more, according to the above equations, the active power is proportionally curtailed, only exploiting β, which is simply defined by the PV module datasheet. Therefore, not only it provides accurate overvoltage and power-sharing control in the same structure, but also its setting is determined with minimum and zero dependencies on the PVG's and MG's parameters, respectively. Based on (10), it does not also need re-tuning when a PVG is installed or isolated, ensuring scalability.

After power curtailment, the proposed method supports a reserve similar to other existing MPPT-based solutions. As displayed in Fig. 5, the MPPT is deactivated in overvoltage conditions. After a demand jump with $\Delta V_{PCC} < 0$, the proposed control is disabled, and the MPPT algorithm is retriggered. Afterward, the PV array voltage moves toward MPP until the PCC voltage restores to the setpoint. This capability highlights both effective control and optimum utilization of PVGs in overvoltage and undervoltage scenarios, respectively.

III. CASE STUDY MICROGRID

To evaluate the effectiveness of the proposed method, a standard 50 Hz, 400 V line-to-line islanded MG with two PV systems is simulated in the RSCAD platform. Fig. 6 and Table 1 present the schematic and detailed parameters of the studied MG, respectively.

As the proposed method controls overvoltage and optimally shares the load power without BESS, load management, and communication link, the case study system compromises only PVGs. This condition is the most extreme scenario for autonomous MG, i.e., it is applicable when the mentioned controllers are included. Similar to existing MPPT-OFF-based solutions [17], [18], [19], [20], [21], [22], [23], [24], [25], this small MG sufficiently simulates different overvoltage case studies in the presence of single and multi PVGs.

The PV array of the 50 kW and 100 kW generators is precisely modeled by single-diode representation [31]. To consider different technologies, monocrystalline and polycrystalline PV modules are connected at the primary source of the first (PVG_1) and second (PVG_2) PV units, respectively. According to the presented information of these PV modules in [32] and [33], β is computed and given in Table 1. The required PV array voltage shift is accordingly computed for PVG_1 and PVG_2 and integrated into their DC/DC converter, i.e., boost and buck, respectively. These converters are equipped with P&O and incremental conductance MPPT algorithms with 0.1 kHz frequency. The DC/AC converter of both PVGs uses the pulse width modulation (PWM) technique in the synchronous reference frame [34]. Since the proposed method supports overvoltage of LV MG based on active power control, reactive power generation and consumption are set to zero for all scenarios. The VSIs are thereby designed to work at unity power factor at STC, 50 and 100 kW for first and second PVGs, respectively.

Finally, constant impedance loads (L_1–L_4) are connected into three PCCs at the nominal voltage level, linked by two lines with Z_L^1 and Z_L^2 impedances. The active power of these purely resistive loads (P_L) is adjusted in the next section to conduct various overvoltage tests.

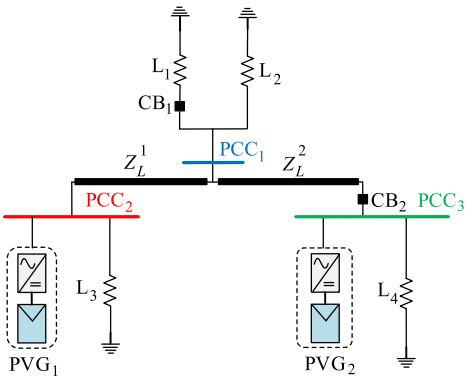

FIGURE 6. Schematic of the standard test microgrid.

TABLE 1. Parameters of the case study microgrid.

Equipment	Description
Lines	Z_L^1 =0.38+j0.05 Ω, Z_L^2 =0.77+j0.1 Ω
Loads	$P_L^1 + P_L^2$ =50 kW (P_L^1 is tunable), P_L^3 =40 kW, and P_L^4 =60 kW (P_L^4 is tunable)
PV systems	PVG_1: 50 kW at STC (Q.PEAK-G4.1 300) V_{OC}=39.7 V, V_{MPP}=32.4 V, I_{SC}=9.8 A, I_{MPP}=9.3 A, β=22.7% DC/DC converter: boost converter, equipped with P&O (0.1 kHz frequency), V_{DC}=1500 V DC/AC converter: PWM (2 kHz frequency)
	PVG_2: 100 kW at STC (YL305P-35b) V_{OC}=46.3 V, V_{MPP}=37.0 V, I_{SC}=8.9 A, I_{MPP}=8.2 A, β=25.1% DC/DC converter: buck converter with incremental conductance (0.1 kHz frequency), V_{DC}=600 V DC/AC converter: PWM (2 kHz frequency)

IV. EVALUATION OF THE PROPOSED METHODOLOGY

This section investigates the authenticity of the proposed method in different load perturbation scenarios in the presence of single and multiple PVGs. Further, an overvoltage event caused by the high PV unit's generation is studied. Table 2 details all these simulated tests in real time. The applied method restores voltage to the nominal value ($V_{PCC,nom} = 1$ pu) when the PCC voltage surpasses 1.1 pu.

A. UNDERLOADING FOR SINGLE-PVG (CASES 1–4)

In the initial study, an overvoltage event due to the underloading is examined for an island with a single PVG. In this regard, an isolated MG incorporating PVG_2 and L_4 is considered. Underloading is yielded at $t = 2$ s by opening CB_2 for $P_L^4 = 80$, 70, and 60 kW, simulating 20, 30, and 40% active power imbalance, respectively. In all these cases, other loads are adjusted so that the initially mentioned MG would be balanced before opening CB_2. The proposed method is also deliberately triggered at $t = 3$ s to show the PCC voltage variation. Fig. 7 depicts the outputs of Case 1, including V_{PV}, PCC voltage at bus 3, and active power waveforms.

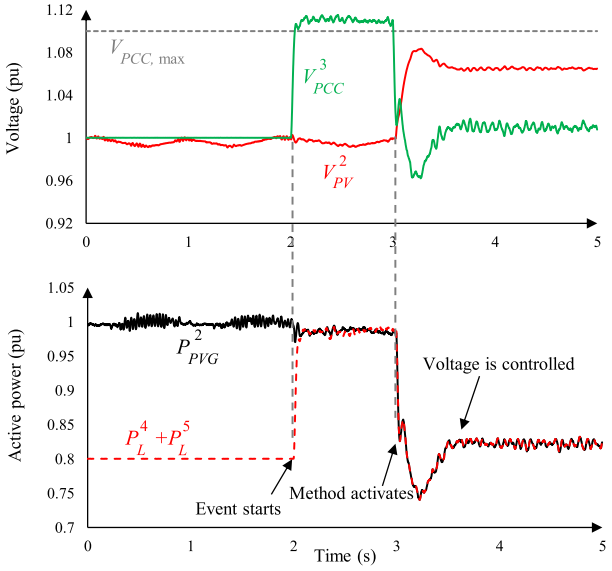

FIGURE 7. Outputs for 20% underloading in Case 1.

It is seen that after 20% underloading, the V_{PCC} at third bus shifts to 1.11 pu ($\Delta V_{PCC} = 0.11$ pu). Through the proposed control method, the PV array operating point shifts from MPP level ($V_{MPP} = 1$ pu) to $V_{NEW} = 1.062$ pu, $\alpha = 6.2\%$. According to (10), the active power of PVG_2 curtails by ∼20% at this new operating point. Hence, the V_{PCC} at bus 3 re-establishes at 1.009 pu within 613 ms, indicating fast and accurate overvoltage regulation.

The test is repeated for 30% and 40% power imbalance in Cases 2 and 3, respectively. The results of these scenarios are illustrated in Fig. 8, wherein the solid and dash lines represent PVG_2 and loads' active power, respectively. It is readily seen that the proposed method controls overvoltage with <2% error within 1s. The controller shows this small error since the presented equations are based on a few simplifications, e.g., considering MPP's right-hand as a linear line. What's more, a greater overvoltage needs more power curtailment which takes a longer time, e.g., especially for Case 3.

As noted earlier, the MPPT algorithm is disabled during the overvoltage situation. The difference between MPP and output powers can be used as a reserve to meet the probable load rise. This capability can be used for stabilizing an MG with an active power shortage. Case 1 is thereby re-simulated while CB_2 is reclosed at $t = 5$ s after voltage regulation.

The outputs in Fig. 9 show that the PCC voltage tends to increase when the load jumps. In this time being, the proposed method is disabled and the PV array moves toward MPP; the reserve power compensates for the power mismatch. Therefore, the PCC voltage restores to the nominal value with the new loading level. This performance elucidates that not only the presented method contributes to overvoltage MG stability, but also it optimizes the PVGs' reserve power in undervoltage (overloading) situations.

TABLE 2. Details of simulated overvoltage scenarios.

Case no.	Scenario description	Underloading level (%)	α_1, α_2 (%)	ΔV_{PCC} (%)	Time (ms)	Voltage error (%)	Max. steady-state power-sharing error (%)
1	Single PVG (opening CB_2)	20	–, 6.2	11.0	613	0.9	–
2		30	–, 9.0	18.1	625	0.8	–
3		40	–, 11.6	26.6	960	1.8	–
4	Single PVG (opening and re-closing CB_2)	20	–, 6.2	11.0	613	0.9	–
5	Multi-PVG (opening CB_1)	20	5.5, 6.2	11.0	554	1.8, 1.7	6.2
6		30	8.0, 9.0	18.1	589	0.8, 0.2	5.1
7	Multi-PVG (opening CB_1 when PVG_1 control is disabled)	20	–, 0.9	11.0	610	0.2, 0.2	–
8	PVG_2 generation rise	20	–, 6.2	11.0	570	0.9	–

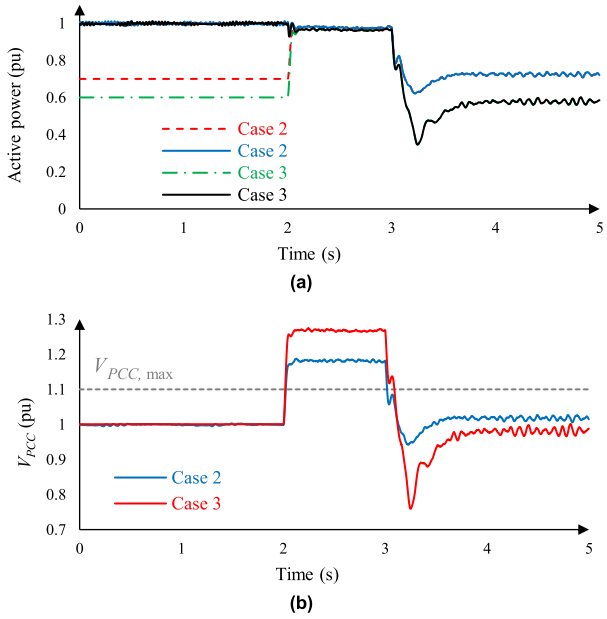

FIGURE 8. Outputs for Cases 2 and 3: a) Active power, b) PCC voltage.

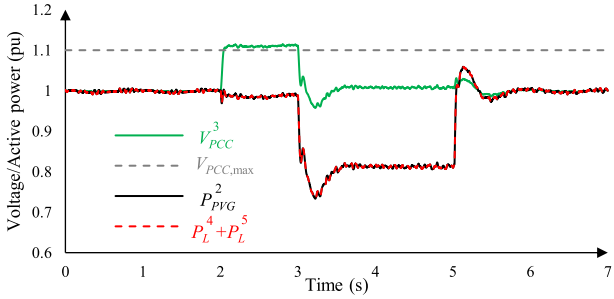

FIGURE 9. Outputs of Case 4 with CB_2 re-closing.

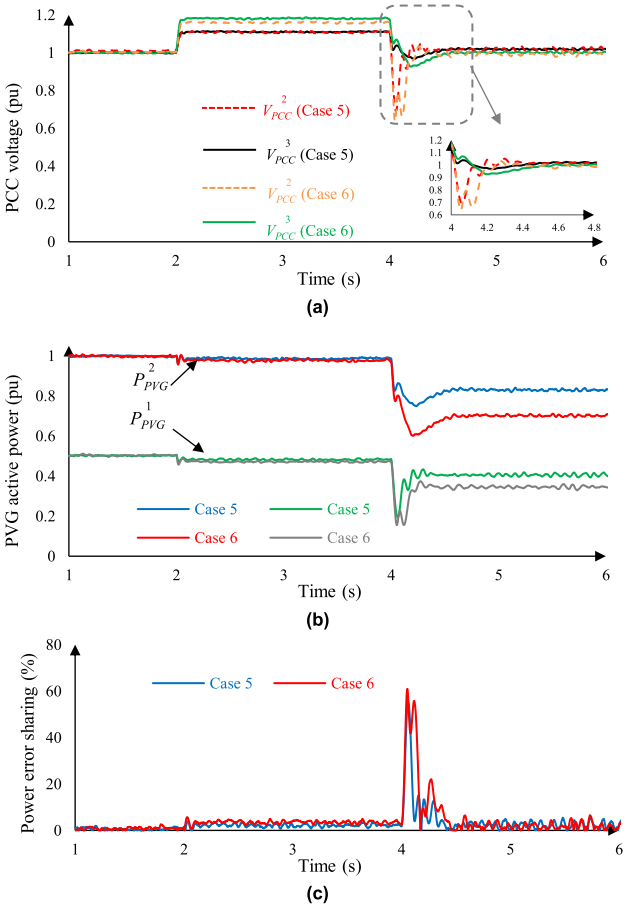

FIGURE 10. Results of multi-PVG in Case 6: a) PCC voltage, b) Active power, c) Power-sharing error.

B. UNDERLOADING FOR MULTI-PVG (CASES 5–7)

To assess the proposed method in multi-PVG cases, L_1 is disconnected at $t = 2$ s in Cases 5 and 6 with 30 and 45 kW power, simulating 20 and 30% power imbalance, respectively. Fig. 10 indicates the outputs, including the PCC voltage at PVGs' buses, active power, and the power-sharing error, i.e., $|P^2_{PVG}(pu) - P^1_{PVG}(pu)|/P^2_{PVG}(pu)$.

It is evident from Fig. 10 (a) that the PCC voltage at all buses is controlled in less than 0.6s. Also, the power-sharing error waveform in Fig. 10 (b) reveals that there is a transient moderate error; nevertheless, it is limited to 6.2% in the steady-state operation.

It is worth noting the results validate the above analytical expressions that this overvoltage control automatically curtails PVGs' active power proportionally. Therefore, both

precise overvoltage and proportional power-sharing are accomplished in the same structure.

In an MG with multiple DGs, it is possible to engage a few PVGs for overvoltage control. This has been demonstrated for the final multi-PVG case whilst the overvoltage control of the first PVG is disabled. The results are displayed in Fig. 11 where $P_L{}^{tot}$ denotes for total load active power.

According to the results, PVG_2 restores the PCC voltage to the nominal level, even when the first PVG controller is deactivated. This highlights the reliable performance of the recommended method, even with a limited number of PVGs contributing to overvoltage control.

C. RISE OF PV SYSTEM GENERATION (CASE 8)

In addition to the low load, high PV generation causes overvoltage incidents. Case 8 is accordingly simulated wherein a generation of PVG_2 in an MG with L_4 increases by raising the received solar irradiance from 800 to 1000 W/m^2 at t =[2–4]s timeframe. The total load at this PCC is 80 kW, i.e., 0 and 20% underloading before and after radiation climb. The proposed method is also activated at $t = 4$ s to illustrate the V_{PCC} and the active power variations.

According to Fig. 12, P^2_{PVG} elevates due to the received irradiance rise; however, it is curtailed by the proposed method in less than 570 ms. Thus, the voltage is restored to the nominal setting, and MG works in a stable operating mode.

According to the results of the analysis, the proposed method effectively stabilizes all overvoltage cases with acceptable power-sharing error within 1 s. This outstanding performance is achieved by exploiting PCC voltage without involving a communication link. In addition, with ease of implementation, this methodology can be thereby integrated into the existing VSIs with minimum effort and cost.

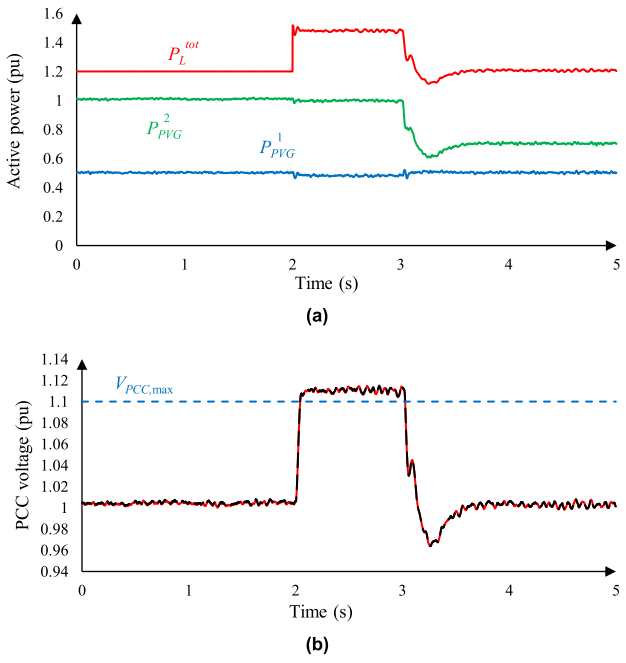

FIGURE 11. Results of overvoltage with 20% active power surplus when PVG_1 overvoltage control is disabled: a) Active power, b) PCC voltage (red dash and black solid lines for PCC voltage at buses 2 and 3).

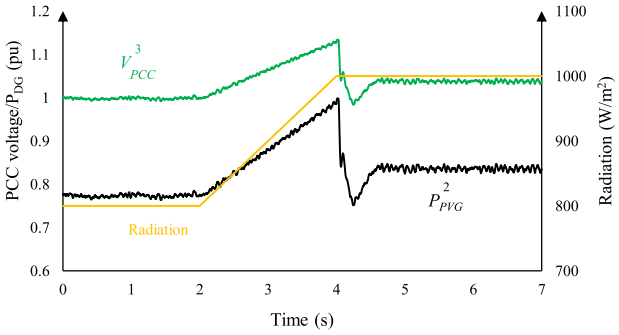

FIGURE 12. Results of overvoltage caused by high PV generation.

V. COMPARISON WITH SOME MPPT-BASED SCHEMES

The overall superior performance of the proposed technique over the existing source-driven MPPT-based schemes is highlighted here through an in-depth comparison. As summarized in Table 3, this comparison reveals several advantages, including:

- First and foremost, the required PV array voltage shift is analytically defined in this work for each PV system regarding its β. Conversely, most existing MPPT-based controllers determined the power curtailment level through simulation [18], [19], [20], [21], [22], [23], [24], [25] or data-driven approaches [14], [28], i.e., lack supporting analytical expressions.
- When a new PV unit is integrated or removed from the MG, existing PVGs do not need re-tuning. This scalability feature has not been supported by the majority of the existing solutions, e.g., [14], [17], [19], and [21].
- The proposed method provides overvoltage control with $<$2% error within 1 s, among the fastest and high accurate solutions. Also, the power-sharing error is $<$6.2% due to the assumptions and simplifications considered in analytical expressions. This power-sharing error can be mitigated/eliminated by optimizing α, i.e., increasing α for a PVG with less contribution in overvoltage control.
- Despite the fast and accurate performance, several schemes suffer high-cost and complex implementation [14], [17], [21], [25], [28], as well as communication dependency [17], [25], [28]. Conversely, the structure of the proposed scheme is straightforward (Fig. 5); it is inexpensively implementable by a sensor, signal generator, and microcontroller/digital signal processor. Also, it only measures PCC voltage deviation for defining α, providing reliable performance without a communication link.
- Dependency on the PV's and MG's characteristics is a paramount feature for the simple development of a

TABLE 3. Comparison of the proposed technique and existing MPPT-OFF-based solutions.

Methodology	Analytical control?	Accuracy	Speed	Power-sharing error	Communication?	Scalability?	ESS/load Support?	PVG/MG Dependency	Cost and Complexity
Over and unbalanced voltage control [17]	Yes	High	Fast	Low	Yes	No	No	Low	High
PV curve estimation and MPPT-OFF [18]	No	High	Fast	Low	No	Yes	No	High	Medium
Control transition mode [19]	No	High	Fast	N/D*	No	No	No	High	Medium
Advanced droop control [20]	No	High	Fast	Low	No	Yes	No	High	Medium
Modified P&O and neural network [21]	No	High	Fast	N/D	No	No	No	High	High
Constant power output [22]	No	High	Fast	N/D	No	Yes	No	High	Medium
PV+BESS [25], [28]	No	High	Fast	Low	Yes	Yes	Yes	Medium	Medium
Neural network + BESS [14]	No	High	Fast	Low	No	No	Yes	High	High
Proposed method	**Yes**	**High**	**Fast**	**Medium**	**No**	**Yes**	**No**	**Low**	**Low**

* N/D: Not Defined

scheme for a new PVG. In this perspective, the settings of the presented MPPT-based schemes in [14], [18], [19], [20], [21], and [22] markedly rely on the parameters of the studied case. This limitation is also a challenge in data-driven approaches, e.g., the number of layers and neurons of the neural network-based method in [14]. Conversely, the presented scheme accepts only the PV array open-circuit voltage ratio to MPP one for β determination, provided in its datasheet. Hence, its dependency on the PVG's and MG's characteristics is limited and zero, respectively.

- Similar to [17], [18], [19], [20], [21], [22], and [23], the current methodology controls overvoltage and proportionally shares the load power without relying on other MG's facilities, while [25] and [28] exploited BESS to fulfill the mentioned goals.

VI. CONCLUSION

Overvoltage is a growing concern in a wide range of low-voltage MGs, e.g., residential and commercial PV systems connected to the distribution network. This paper presents a new power-sharing-based overvoltage control method for PV-based LV islanded MG. This methodology employs a disturbance into the PV array voltage, shifting it to the right-hand side of MPP. Unlike the existing MPPT-based schemes, the size of this voltage shift is analytically quantified in terms of overvoltage level. As another advantage, the power curtailment is determined with respect to the PVG MPP power, i.e., the curtailed power is defined proportionally. Hence, accurate power-sharing is achieved in the same control structure. Furthermore, this analytical formula does not need re-setting after the MG structure is changed, e.g., when a new PVG is installed or disconnected.

The proposed method is assessed in RTDS, taking precise modeling for the PV array and VSI into account. This analysis corroborates the accurate and timely overvoltage control and power-sharing of this method under various scenarios. Unlike several existing solutions, this outstanding performance does not depend on the PV array technology, MPPT algorithm, and DC/DC converter topologies. It is also unveiled that accurate overvoltage control is ensured even when a few PVGs are equipped with the proposed strategy.

Similar to the existing works in the literature, this methodology does not support the PVG operation under partial shading. The improvement of the proposed method to fill this gap is considered for future work.

According to the mentioned advances and the simple and inexpensive structure of the proposed method, it is an effective solution for practical PV-based LV islanded MGs.

REFERENCES

[1] M. H. Saeed, W. Fangzong, B. A. Kalwar, and S. Iqbal, "A review on microgrids' challenges & perspectives," *IEEE Access*, vol. 9, pp. 166502–166517, 2021, doi: 10.1109/ACCESS.2021.3135083.

[2] M. Farrokhabadi, "Microgrid stability definitions, analysis, and examples," *IEEE Trans. Power Syst.*, vol. 35, no. 1, pp. 13–29, Jan. 2020, doi: 10.1109/TPWRS.2019.2925703.

[3] *IEEE Standard Conformance Test Procedures for Equipment Interconnecting Distributed Energy Resources with Electric Power Systems and Associated Interfaces*, Standard 1547.1, 2020, doi: 10.1109/IEEESTD.2020.9097534.

[4] N. T. Mbungu, A. A. Ismail, M. AlShabi, R. C. Bansal, A. Elnady, and A. K. Hamid, "Control and estimation techniques applied to smart microgrids: A review," *Renew. Sustain. Energy Rev.*, vol. 179, Jun. 2023, Art. no. 113251, doi: 10.1016/j.rser.2023.113251.

[5] S. Li, A. Oshnoei, F. Blaabjerg, and A. Anvari-Moghaddam, "Hierarchical control for microgrids: A survey on classical and machine learning-based methods," *Sustainability*, vol. 15, no. 11, p. 8952, Jun. 2023, doi: 10.3390/su15118952.

[6] J. Duarte, M. Velasco, P. Martí, A. Camacho, J. Miret, and C. Alfaro, "Decoupled simultaneous complex power sharing and voltage regulation in islanded AC microgrids," *IEEE Trans. Ind. Electron.*, vol. 70, no. 4, pp. 3888–3898, Apr. 2023, doi: 10.1109/TIE.2022.3179553.

[7] J. A. S. Neto, A. C. Z. De Souza, E. V. De Lorenci, T. P. Mendes, P. M. D. D. Santos, and B. D. N. Nascimento, "Static voltage stability analysis of an islanded microgrid using energy function," *IEEE Access*, vol. 8, pp. 201005–201014 2020, doi: 10.1109/ACCESS.2020.3036107.

[8] M. H. Elkholy, H. Metwally, M. A. Farahat, T. Senjyu, and M. E. Lotfy, "Smart centralized energy management system for autonomous microgrid using FPGA," *Appl. Energy*, vol. 317, Jul. 2022, Art. no. 119164, doi: 10.1016/j.apenergy.2022.119164.

[9] S. Das, I. U. Nutkani, and C. A. Teixeira, "Decentralized master–slave control for series-cascaded islanded AC microgrid," *IEEE Trans. Ind. Electron.*, vol. 69, no. 6, pp. 5942–5951, Jun. 2022, doi: 10.1109/TIE.2021.3094414.
[10] F. Guo, L. Wang, C. Wen, D. Zhang, and Q. Xu, "Distributed voltage restoration and current sharing control in islanded DC microgrid systems without continuous communication," *IEEE Trans. Ind. Electron.*, vol. 67, no. 4, pp. 3043–3053, Apr. 2020, doi: 10.1109/TIE.2019.2907507.
[11] S. Ullah, L. Khan, I. Sami, and N. Ullah, "Consensus-based delay-tolerant distributed secondary control strategy for droop controlled AC microgrids," *IEEE Access*, vol. 9, pp. 6033–6049, 2021, doi: 10.1109/ACCESS.2020.3048723.
[12] L. Jia, S. Pannala, G. Kandaperumal, and A. Srivastava, "Coordinating energy resources in an islanded microgrid for economic and resilient operation," *IEEE Trans. Ind. Appl.*, vol. 58, no. 3, pp. 3054–3063, May 2022, doi: 10.1109/TIA.2022.3154337.
[13] F. Barati, B. Ahmadi, and O. Keysan, "A hierarchical control of supercapacitor and microsources in islanded DC microgrids," *IEEE Access*, vol. 11, pp. 7056–7066, 2023, doi: 10.1109/ACCESS.2023.3237684.
[14] D.-D. Zheng, S. S. Madani, and A. Karimi, "Data-driven distributed online learning control for islanded microgrids," *IEEE J. Emerg. Sel. Topics Circuits Syst.*, vol. 12, no. 1, pp. 194–204, Mar. 2022, doi: 10.1109/JETCAS.2022.3152938.
[15] E. Rokrok, M. Shafie-Khah, and J. P. S. Catalão, "Review of primary voltage and frequency control methods for inverter-based islanded microgrids with distributed generation," *Renew. Sustain. Energy Rev.*, vol. 82, pp. 3225–3235, Feb. 2018, doi: 10.1016/j.rser.2017.10.022.
[16] *IEA, Solar PV Power Capacity in the Net Zero Scenario, 2015–2030*. [Online]. Available: www.iea.org/data-and-statistics/charts/solar-pv-power-capacity-in-the-net-zero-scenario-2015-2030
[17] A. R. Vadavathi, G. Hoogsteen, and J. L. Hurink, "PV inverter based fair power quality control," *IEEE Trans. Smart Grid*, vol. 14, no. 5, pp. 3776–3790, Sep. 2023, doi: 10.1109/TSG.2023.3244601.
[18] Z. Wang, H. Yi, Y. Jiang, Y. Bai, X. Zhang, F. Zhuo, F. Wang, and X. Liu, "Voltage control and power-shortage mode switch of PV inverter in the islanded microgrid without other energy sources," *IEEE Trans. Energy Convers.*, vol. 37, no. 4, pp. 2826–2836, Dec. 2022, doi: 10.1109/TEC.2022.3188334.
[19] V. F. Pires, A. Cordeiro, D. Foito, and J. F. Silva, "Control transition mode from voltage control to MPPT for PV generators in isolated DC microgrids," *Int. J. Electr. Power Energy Syst.*, vol. 137, May 2022, Art. no. 107876, doi: 10.1016/j.ijepes.2021.107876.
[20] W. Zhang, Z. Zheng, and H. Liu, "Droop control method to achieve maximum power output of photovoltaic for parallel inverter system," *CSEE J. Power Energy Syst.*, vol. 8, no. 6, pp. 1636–1645, Nov. 2022, doi: 10.17775/CSEEJPES.2020.05070.
[21] S. R. and H. S., "Active power control of a photovoltaic system without energy storage using neural network-based estimator and modified P&O algorithm," *IET Gener., Transmiss. Distrib.*, vol. 12, no. 4, pp. 927–934, Feb. 2018, doi: 10.1049/iet-gtd.2017.0156.
[22] H. D. Tafti, A. I. Maswood, G. Konstantinou, J. Pou, and F. Blaabjerg, "A general constant power generation algorithm for photovoltaic systems," *IEEE Trans. Power Electron.*, vol. 33, no. 5, pp. 4088–4101, May 2018, doi: 10.1109/TPEL.2017.2724544.
[23] Z. Chen, R. H. Lasseter, and T. M. Jahns, "Active power reserve control for grid-forming PV sources in microgrids using model-based maximum power point estimation," in *Proc. IEEE Energy Convers. Congr. Expo. (ECCE)*, Sep. 2019, pp. 41–48, doi: 10.1109/ECCE.2019.8913174.
[24] M. S. H. Lipu, S. Ansari, M. S. Miah, K. Hasan, S. T. Meraj, M. Faisal, T. Jamal, S. H. M. Ali, A. Hussain, K. M. Muttaqi, and M. A. Hannan, "A review of controllers and optimizations based scheduling operation for battery energy storage system towards decarbonization in microgrid: Challenges and future directions," *J. Cleaner Prod.*, vol. 360, Aug. 2022, Art. no. 132188, doi: 10.1016/j.jclepro.2022.132188.
[25] Y. Xia, M. Yu, P. Yang, Y. Peng, and W. Wei, "Generation-storage coordination for islanded DC microgrids dominated by PV generators," *IEEE Trans. Energy Convers.*, vol. 34, no. 1, pp. 130–138, Mar. 2019, doi: 10.1109/TEC.2018.2860247.
[26] Z. Zhang, C. Dou, D. Yue, Y. Xue, X. Xie, C. Deng, and B. Zhang, "Voltage sensitivity-related hybrid coordinated power control for voltage regulation in ADNs," *IEEE Trans. Smart Grid*, early access, Jul. 6, 2023, doi: 10.1109/TSG.2023.3292939.
[27] Z. Zhang, C. Dou, D. Yue, Y. Zhang, B. Zhang, and Z. Zhang, "Event-triggered hybrid voltage regulation with required BESS sizing in high-PV-penetration networks," *IEEE Trans. Smart Grid*, vol. 13, no. 4, pp. 2614–2626, Jul. 2022, doi: 10.1109/TSG.2022.3168440.
[28] Z. Huang, Y. Li, X. Cheng, and M. Ke, "A voltage-shifting-based state-of-charge balancing control for distributed energy storage systems in islanded DC microgrids," *J. Energy Storage*, vol. 69, Oct. 2023, Art. no. 107861, doi: 10.1016/j.est.2023.107861.
[29] L.-L. Fan, V. Nasirian, H. Modares, F. L. Lewis, Y.-D. Song, and A. Davoudi, "Game-theoretic control of active loads in DC microgrids," *IEEE Trans. Energy Convers.*, vol. 31, no. 3, pp. 882–895, Sep. 2016, doi: 10.1109/TEC.2016.2543229.
[30] F.-J. Lin, K.-H. Tan, C.-F. Chang, M.-Y. Li, and T.-Y. Tseng, "Development of intelligent controlled microgrid for power sharing and load shedding," *IEEE Trans. Power Electron.*, vol. 37, no. 7, pp. 7928–7940, Jul. 2022, doi: 10.1109/TPEL.2022.3152167.
[31] K. Tifidat and N. Maouhoub, "An efficient method for predicting PV modules performance based on the two-diode model and adaptable to the single-diode model," *Renew. Energy*, vol. 216, Nov. 2023, Art. no. 119102, doi: 10.1016/j.renene.2023.119102.
[32] *Q.PEAK-G4.1 300 Datasheet*. [Online]. Available: www.qcells.co.uk/uploads/tx_abdownloads/files/Hanwha_Q_CELLS_Data_sheet_QPEAK-G4.1_300-310_2017-11_Rev01_EN.pdf
[33] *YL305P-35b Datasheet*. [Online]. Available: www.enfsolar.com/pv/panel-datasheet/crystalline/31539
[34] M. Morey, N. Gupta, M. M. Garg, and A. Kumar, "A comprehensive review of grid-connected solar photovoltaic system: Architecture, control, and ancillary services," *Renew. Energy Focus*, vol. 45, pp. 307–330, Jun. 2023, doi: 10.1016/j.ref.2023.04.009.

REZA BAKHSHI-JAFARABADI (Member, IEEE) received the degree from the Ferdowsi University of Mashhad, Mashhad, Iran. As a Postdoctoral Researcher, he rejoins intelligent electrical power grids (IEPG) with TU Delft, Delft, The Netherlands, in 2022. His research interests include renewable energy technologies, integration of distributed generators to the power systems, microgrid protection, and HVDC systems. He is a member of Cigre and actively participated in WG B5.83. He is also an Associate Editor of *e-Prime—Advances in Electrical Engineering, Electronics and Energy* (Elsevier).

ALEKSANDRA LEKIĆ (Senior Member, IEEE) received the B.Sc., M.Sc., and Ph.D. degrees in electrical engineering from the School of Electrical Engineering, University of Belgrade, Serbia, in 2012, 2013, and 2017, respectively. Between 2012 and 2018, she has been a Teaching Assistant with the School of Electrical Engineering, University of Belgrade, and an Assistant Professor, from 2018 to 2019. In 2019, she was a Postdoctoral Researcher with the Department of Electrical Engineering (ESAT), KU Leuven, and the Institute EnergyVille, Genk, Belgium. Since January 2020, she has been a tenured Assistant Professor with the Group of Intelligent Electrical Power Grids, Faculty of Electrical Engineering, Mathematics and Computer Science, TU Delft. She leads a team of researchers specializing in the control of HVDC/AC power systems. She is also an Associate Editor of the *International Journal of Electrical Power & Energy Systems* (Elsevier) and *Journal of Electrical Engineering* (Springer). She represents TU Delft in the General Assembly in the CRESYM Organization, committed to open-source software development for the electrical grids.

FARZAD DEHGHAN MARVASTI (Member, IEEE) received the Ph.D. degree in electrical engineering from Yazd University, Yazd, Iran. He is currently a Postdoctoral Research Fellow with the Intelligent Electrical Power Grids Group (IEPG), Delft University of Technology, Delft, The Netherlands. His major research interest includes control and protection of multi-terminal HVDC grids.

JOSE DE JESUS CHAVEZ (Senior Member, IEEE) received the M.Sc. and Ph.D. degrees from the Center for Research and Advanced Studies, National Polytechnic Institute, Mexico City, in 2006 and 2009, respectively. In 2009, he joined the RTX-LAB, University of Alberta, as a Visiting Ph.D. Student. He joined the Technological Institute of Morelia, Mexico, as an Assistant Professor, in 2010, where he was a Full Professor, in 2012, and the Chair of the Graduate and Research Program in electrical engineering, from 2014 to 2016. He was a Postdoctoral Member with TU Delft, The Netherlands, from 2016 to 2020, and has been a Guest Researcher, since 2021. He joined the National Technological Institute of Mexico (TecNM), from 2020 to 2022. Since 2023, he has been a Professor with the School of Engineering and Sciences, Guadalajara Campus, Tecnologico de Monterrey. His research interests include primary protection, wide area protection, digital protective relays, and real time simulation. He is an Associate Editor of *e-Prime—Advances in Electrical Engineering, Electronics and Energy* (Elsevier).

MARJAN POPOV (Fellow, IEEE) received the Ph.D. degree in electrical power engineering from the Delft University of Technology, Delft, in 2002. He is currently a Professor in power system protection. He is also a Chevening Alumnus and, in 1997, he was an Academic Visitor with the University of Liverpool, Liverpool, U.K., working with the arc research group on modeling SF6 circuit breakers. His research interests include future power systems, large-scale power system transients, intelligent protection for future power systems, and wide-area monitoring and protection. He is a member of Cigre and actively participated in WG C4.502 and WG A2/C4.39. In 2010, he received the prestigious Dutch Hidde Nijland Prize for extraordinary research achievements. He was a recipient of the IEEE PES Prize Paper Award and IEEE Switchgear Committee Award, in 2011. He is the Co-Editor-in-Chief of *e-Prime—Advances in Electrical Engineering, Electronics and Energy* (Elsevier) and an Associate Editor of *International Journal of Electrical Power and Energy Systems* (Elsevier). In 2017, together with the Dutch utilities TenneT, Alliander, and Stedin, he founded the Dutch Power System Protection Centre to promote research and education in power system protection.